

*Поставлені експериментальні дослідження по моделюванню радіально-ротаційного профілювання сталевих ободів коліс транспортних засобів різних типорозмірів. Встановлені інтегральні меридіональні, тангенціальні і радіальні деформації. На їх основі розраховано ресурс пластичності, визначено напружений стан, а також інтенсивності деформацій і напружень для різних ділянок профілю обода колеса. Проведено порівняння двох існуючих схем профілювання*

*Ключові слова: обід колеса, напруження, деформації, радіально-ротаційне профілювання, метод сіток, темплет, ресурс пластичності*

*Поставлены экспериментальные исследования по моделированию радиально-ротационного профилирования стальных ободьев колес транспортных средств различных типоразмеров. Установлены интегральные меридиональные, тангенциальные и радиальные деформации. На их основе рассчитан ресурс пластичности, определено напряженное состояние, а также интенсивности деформаций и напряжений для различных участков профиля обода колеса. Проведено сравнение двух существующих схем профилирования*

*Ключевые слова: обод колеса, напряжения, деформации, радиально-ротационное профилирование, метод сеток, темплет, ресурс пластичности*

UDC 621.983.044  
DOI: 10.15587/1729-4061.2016.76225

# DETERMINING EXPERIMENTALLY THE STRESS-STRAINED STATE IN THE RADIAL ROTARY METHOD OF OBTAINING WHEELS RIMS

**R. Puzyr**

PhD, Associate Professor\*  
E-mail: puzyruslan@gmail.com

**T. Haikova**

PhD\*  
E-mail: tanyahaikova@mail.ru

**O. Trotsko**

PhD, Associate Professor\*  
E-mail: trotsko@kdu.edu.ua

**R. Argat**

Senior Lecturer\*  
E-mail: argat@ua.fm

\*Department of engineering technology  
Kremenchuk Mykhailo Ostrohradskyi National University  
Pershotravneva str., 20, Kremenchuk, Ukraine, 39600

## 1. Introduction

The majority of the steel wheels of transportation vehicles consist of the disk, welded to the rim, onto which a tire is mounted. And while the technology of manufacturing the wheels disks by the methods of sheet stamping is explored quite well, the questions concerning the radial rotary profiling as one of the progressive methods of manufacturing the rims, remain insufficiently examined and open [1, 2].

The quality of wheels affects not only the comfort of motion and work in a transportation vehicle, but also inertial characteristics of automobile, fuel economy, operation reliability, as well as safety.

The quality of the steel rims of wheels can be increased by improving the technologies of their production, but improvement in technologies is unthinkable without thorough study of the processes and phenomena that occur in the manufacturing cycle, in the deformation area, taking into account the limiting factors and applying accumulated engineering and scientific and technical information. The relevance of this work is in thorough study of the field of deformation and stresses, determining their magnitude and direction that occur in a workpiece in all transitions of pro-

filming the rims of wheels, detection of zones of localization of the deformations to form technological methods on selection of metal in the critical sections of the rim.

## 2. Literature review and problem statement

The complexity of experimental and theoretical analysis of the radial rotary profiling of the rims of wheels is noted by many authors of the studies on the discussed topic [1–4], and for now there are no clear recommendations on determining the main indicators of the stress-strained state with regard to locality of the load application. Thus, the article [5] provides qualitative characteristics in connection to the distribution of deformations and stresses in the different sections of the wheel's profile but the information about the method of their determining and the data on their quantitative assessment are absent. In the papers [1–3], the stress-strained state was determined by the method of tensometry, by gluing the sensors on a workpiece in the tested zone. For registering indications of tensoresistors, they used expensive high-precision equipment of the analog-to-digital type of converters and operational amplifiers. However, this method is connected

with a large quantity of measurements and requires precise calibration of tensoresistors and skilled researchers. The interpretation of the results by some authors [1, 2] may differ radically from that of others [3]. At the same time, practical results of these articles are of particular nature, they can be used for specified wheels and, therefore, the authors themselves expressed a wish about necessity of conducting studies for other standard sizes.

The studies of various authors [3, 6–9] are in a larger degree directed toward the simulation of the process of profiling with the aid of applied program complexes, conducting simulation experiments and obtaining data of numerical calculations, which is connected to accepting specific simplifications and hypotheses. Thus, in the article [3], the zones of effects of the largest radial deformations are determined; in the papers [6, 8], the empirical dependencies are brought out, which establish the connection of thinning the metal to its mechanical characteristics and geometry of the deforming tool. The article [7] defines optimal geometric dimensions of the workpiece for specific standard size of the rim, while [9] provides general approaches to numerical simulation of the processes of cold forming. But the authors of the mentioned papers assert that it is necessary to perform physical experiments for checking their results.

That is why, to examine the process of radial rotary profiling, its intensification, it is necessary to conduct experimental studies on the models under laboratory conditions, with the use of contemporary measuring and registering equipment. This will increase the quality and accuracy of obtained data and will confirm or refute the existing results.

### 3. The purpose and objectives of the study

The purpose of experimental studies was determining the stress-strained state when profiling of the rims of wheels, as well as defining the intensity of deformations, stresses and the resource of plasticity.

To achieve this goal, the following tasks were set:

- to determine maximal total deformations in each transition of the radial-rotary profiling of the rims of wheels;
- to define the number of the transition of profiling, in which the semifinished product is exposed to the effect of the largest compressive radial deformations;
- to compare two schemes of profiling, based on which to select the most rational one by the criterion of variation in thickness;
- to prepare general recommendations on the improvement and intensification of the technology of radial rotary profiling of the rims of wheels.

### 4. Materials and methods of experimental studies of the stress-strained state during profiling

The strained state was determined by the method of coordinate grids on the models of the rims of wheels with the scale factor 1:4. Standard representatives of the narrow-profile and wide-profile rims of the wheels were examined: 4.5Ex16; W8x16; 5.5Fx20; DW14Lx38; DW20Ax26; 9.00x22.5.

For conducting the experiments, the following simplifications were accepted:

- hypothesis on isotropism and incompressibility of material;

- hypothesis on the uniformity of deformation within each cell;

- the process is close to monotonic deformation and, therefore, it is possible to use the positions of deformation theory of plasticity;

- a workpiece is under conditions of the flat stressed and volumetric strained state;

- elastic deformations are the magnitudes of the higher order of smallness compared to plastic and are not considered in the calculations;

- strain components were conditionally accepted as average and were related to the cell center.

Dividing grids were applied to the plane of rectangular sample by a special device that consists of the cutter, rigid lath and the base, which was placed in the spindle of the vertical milling machine 6R12, while the workpieces were fixed by seizures on the coordinate table; the mechanisms of positioning the machine permit error of 0.01 mm. Then the strip was twisted into the cowling and was butt-welded. The family of coordinate lines formed a coordinate grid with the square cells on the surface of the workpiece. The sizes of square cells were 3×3 mm. The workpiece of a wheel rim with the coordinate grid, marked on it, is shown in Fig. 1.



Fig. 1. Model of a workpiece for the wheel rim with the family of coordinate lines

The set of workpieces for studying the stress-strained state in each transition of the process of radial-rotary profiling is shown in Fig. 2.



Fig. 2. Set of experimental samples

Processing the experimental information, obtained by the method of coordinate grids, remains quite labor-consuming process, which is predetermined by a large number of measuring operations. That is why, for processing experimental data we used visualization of initial information with the help of applied programs of three-dimensional simulation, which made it possible to simplify measuring the coordinates of initial and deformed grids and to partially automate the process of computing the displacements and deformations by the tools of utilized software. For minimization of errors of measurement in the coordinate grids, we used the program package KOMPAS 3D V13 by the company Ascon.

Material of the models of the workpieces of the rims – steel 1008 (08F China).

Sizes of the models of workpieces for the rims of wheels:

W8x16 –  $h = 1.2 \text{ mm}$ ,  $D = 100 \text{ mm}$ ,  $l = 68 \text{ mm}$ ;

4.5Ex16 –  $h = 0.8 \text{ mm}$ ,  $D = 100 \text{ mm}$ ,  $l = 46 \text{ mm}$ ;

5.5Fx20 –  $h = 1 \text{ mm}$ ,  $D = 125 \text{ mm}$ ,  $l = 54 \text{ mm}$ ;

DW14Lx38 –  $h = 1.25 \text{ mm}$ ,  $D = 230 \text{ mm}$ ,  $l = 115 \text{ mm}$ ;

DW20Ax26 –  $h = 1.4 \text{ mm}$ ,  $D = 145.5 \text{ mm}$ ,  $l = 156 \text{ mm}$ ;

9.00x22.5 –  $h = 1.75 \text{ mm}$ ,  $D = 130 \text{ mm}$ ,  $l = 77.5 \text{ mm}$ ;

where  $h$ ,  $D$  and  $l$  are the thickness, diameter and length of the sample, respectively.

External (1) and internal (2) rollers for profiling the rims of wheels of all enumerated standard sizes to the 1:4 scale were designed and manufactured from steel 45, taking into account profiling on the lathe, as well as the mount (3) with the axis (4) for external rollers (1) were designed and produced (Fig. 3).

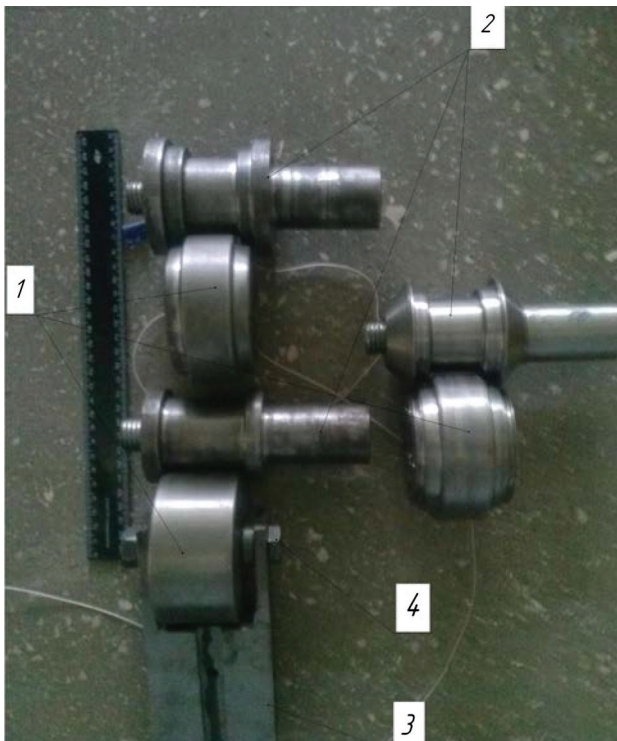


Fig. 3. Set of deforming rollers for profiling of the rim 4.5Ex16

The die for sagging of the cowling was designed and manufactured (Fig. 4).

The workpiece was upset in the die in the tensile testing machine UME-10TM from two sides simultaneously, after which it was placed on the internal roller, fixed in the chuck

of the lathe. Internal roller was fastened into the chuck of the lathe, and the assembled mount was pressed in the cutter holder (Fig. 5).



Fig. 4. Distribution of the workpiece by conical punches



Fig. 5. Installation for profiling the rims of wheels on the lathe

External roller was moved to the internal until joining the workpiece. After the joining, the internal roller was set into rotary motion and the external, fixed in the cutter holder, into progressive motion of transition. Thus occurred the process of profiling the wheel rim. As the result of experiments, we obtained the rims of the wheels of all standard sizes to scale 1:4, in full compliance with technical requirements (Fig. 6).



Fig. 6. Profiles of the models of the rims of wheels in the transitions of radial-rotary profiling for the standard size 5.5Fx20

For each type of the wheel rim, we carried out 6 experiments in each transmission of profiling and distribution, after which the templets were cut out of the obtained semifinished products to study the distortions of dividing grid in the transitions (Fig. 7).





Fig. 7. Templets in the transitions of profiling for the model of the wheel rim 5.5Fx20

The cut-out templets were photographed with identical focal length and uploaded into the window of the program KOMPAS 3D V13, where the points were marked in the grid nodes and the distances were measured between them in the meridional and tangential direction by the tools of the software program.

### 5. Results of studies on the simulation of the process of profiling the rims of wheels

In the deformation area there occurs, besides normal, shearing stresses as well, caused by the effect of local load and by asymmetry of the deformation area. The action of shearing stresses, which are accompanied by shearing strains, must cause distortion of the dividing grid, which is manifested in the transformation of initial square into the parallelogram. However, measurement of the angles of cells after loading by transitions demonstrated that the angles between the intersected sides remain within the range of  $90^\circ \pm 2^\circ$ . This is, obviously, linked to the phenomenon, in accordance with which the shearing stresses in geometric center of the local deformation area are equal to zero, and since the entire perimeter of the workpiece consecutively appears in the center of the area of plastic deformation, where the tangential and meridional stresses, the largest in magnitude, act, then the distortions of the cells in the form of turns disappear and the resulting grid acquires the form of rectangles (Fig. 8).

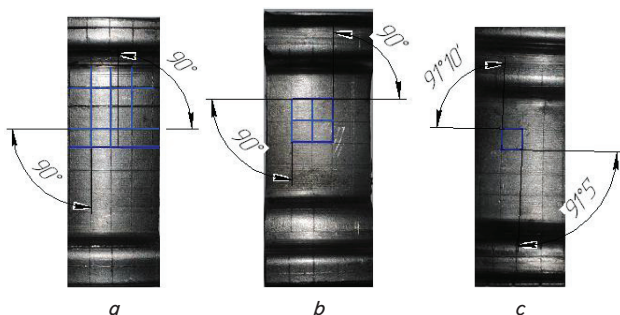


Fig. 8. Templets by the transitions of profiling with the rectangular deformed grid: a — the first transition; b — the second transition; c — the third transition

Since the undistorted grid had a form of square cell before the deformation, in which it was possible to enter a circle, then for calculating the main logarithmic deformations in the transitions, it is possible to use the dependencies [10]

$$\left. \begin{aligned} \epsilon_r &= \ln \frac{r_1}{r_0}, \\ \epsilon_\theta &= \ln \frac{r_2}{r_0}, \end{aligned} \right\} \quad (1)$$

where  $r_0$ ,  $r_1$  and  $r_2$  are the radius of circle and the principal axes of ellipsis, respectively.

The third component of true deformations was found from the condition of volume constancy without taking into account the signs of the deformations [10]

$$\epsilon_m + \epsilon_\theta + \epsilon_r = 0, \quad (2)$$

where  $\epsilon_r$  is the logarithmic deformation by the thickness of a semifinished product.

For the selected templet, the measurements were averaged in each section of the profile of the rim, and then we found the mean arithmetic value of deformation for the entire sample in each zone of measurement (Fig. 9).

Thus, the calculations were produced for the entire nomenclature of the models of standard sizes of the rims of wheels, indicated above, for each transition of radial-rotary profiling. The standard results data of the study are presented in Fig. 10.

The results of measurements for each standard size of the model of the rim and transition of radial-rotary profiling were statistically processed according to the method DSTU 8.207-76. The normality of the results distribution of experimental data was confirmed, as well as their reproducibility, by the Cochran criterion (level of significance  $q = 0.05$ ).

The strained state of the studied sections in transitions was evaluated by the intensity of logarithmic deformations [12]

$$\epsilon_i = \frac{2}{\sqrt{3}} \sqrt{\epsilon_m^2 + \epsilon_m \epsilon_\theta + \epsilon_\theta^2}. \quad (3)$$

The connection between the intensity of stresses and intensity of deformations, as well as the tensile strength, was determined with the use of regression dependencies [13] or using the diagrams of plasticity [17]

$$\sigma_i = \sigma_s = \sigma_{s0} + 3.4 \epsilon^{0.6} \quad (4)$$

$$\sigma_b = \sigma_{b0} + 1.6 \epsilon^{0.76}, \quad (5)$$

where  $\sigma_{s0}$ ,  $\sigma_{b0}$  are the first member of equations, which characterizes initial mechanical properties;  $\epsilon$  are the intensities of true deformations.

The index of the stress-strained state was calculated by the formula [12]

$$\eta = \frac{(\epsilon_r + 2\epsilon_\theta)}{(2\epsilon_r + \epsilon_\theta)}. \quad (6)$$

Using the value  $\eta$ , we calculated the critical intensity of logarithmic deformations for this stressed state by the formula, received from the condition of loss of stability [12]

$$\epsilon_p = \frac{2\sqrt{1-\eta+\eta^2}}{2-\eta}, \quad (7)$$

where  $n$  is the indicator of strengthening, determined by mechanical characteristics of the used metal [14].

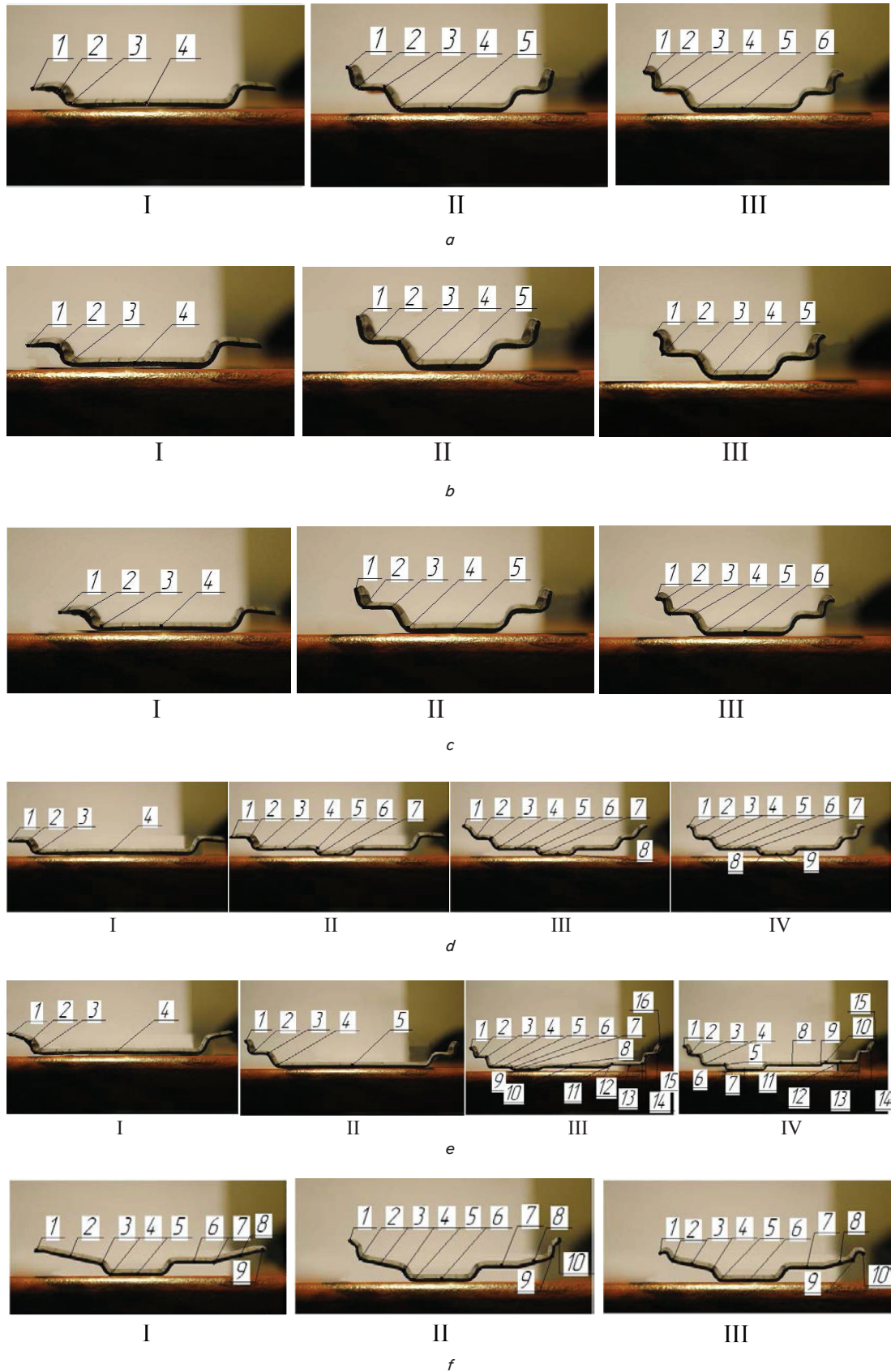


Fig. 9. Transitions of profiling the models of the rims of wheels (I, II, III, IV — the first, second, third and fourth transitions, respectively): *a* — W8x16; *b* — 4.5Ex16; *c* — 5.5Fx20; *d* — DW14Lx38; *e* — DW20Ax26; *f* — 9.00x22.5; 1 — zone of lateral flange, 2 — coupling of the wall of flange with the shelf, 3 — coupling of the shelves with the walls of additional stream, 4 — coupling of the walls of additional stream and additional stream, 5 — zone of shelves, 6 — coupling of the zone of shelves with the walls of central stream, 7 — coupling of the walls of central stream with the central stream, 8 — zone of central stream, 9–16 — the same zones for asymmetrical profile DW20Ax26, respectively

Further on, the used resource of plasticity for each section of the templet in the transitions of profiling was determined, using the criterion of V. A. Ogorodnikov [11]

$$\psi = \int_0^{\varepsilon_{\text{p}}} \left( 1 + 0.2 \arctg \frac{d\eta}{d\varepsilon_i} \right) \frac{\varepsilon_i^{0.2 \arctg \frac{d\eta}{d\varepsilon_i}}}{\left[ \varepsilon_p \right]^{1 + 0.2 \arctg \frac{d\eta}{d\varepsilon_i}}} d\varepsilon_i. \quad (8)$$

Fig. 10, 11 demonstrate the standard graphs of distribution of logarithmic deformations in the transitions of profiling and intensity of stresses and strains, as well as the used plasticity limit, respectively, for the standard size of the wheel rim DW14Lx38, which are built according to the results of processing experimental information in the MathCAD program [14].

The data analysis of graphs on the distribution of logarithmic deformations revealed that the deformations are distributed along the sections of the profile extremely unevenly in all transitions of profiling for each standard size of the rim. Thus, for the profiles W8x16, 4.5Ex16, 5.5Fx20, the strains distribution along the entire profile of the rim has practically similar nature, although their magnitude for each standard size differs slightly, which is obviously connected with the different ratio of the width of wheel to the diameter and different schemes of deformation.

### 6. Discussion of the results of experimental study on determining main characteristics of the stress-strained state when profiling the rims of wheels

In the first transition, the largest meridional deformations occur in section 3 (coupling of central stream and wall) and are equal to (+14 %), (+13 %), (+12 %) for the rims of wheels W8x16, 4.5Ex16, 5.5Fx20, respectively. The largest radial deformations – in section 3: (–10 %), (–15 %), (–13 %); the largest tangential deformations – in section 4 (zone of central stream): (–4.1 %), (–4.0 %), (–3.8 %).

The obtained data confirm similar studies on the measurement of deformations, which were cited above [1–5], but they were carried out under manufacturing conditions on the full-scale models of the rims. The places of radius transitions undergo the effect of the largest stretching deformations, where their localization takes place, which leads to local thinning of metal in these zones. Bastings of board flanges (zones 1, 2, Fig. 9, a–c) obtain tensile deformations in the tangential and meridional direction and compressions in the radial, which leads to thinning of metal in these zones. Section 4 is deformed with elongation in the meridional and radial directions and with compression in the tangential, which leads to insignificant thickening of this zone.

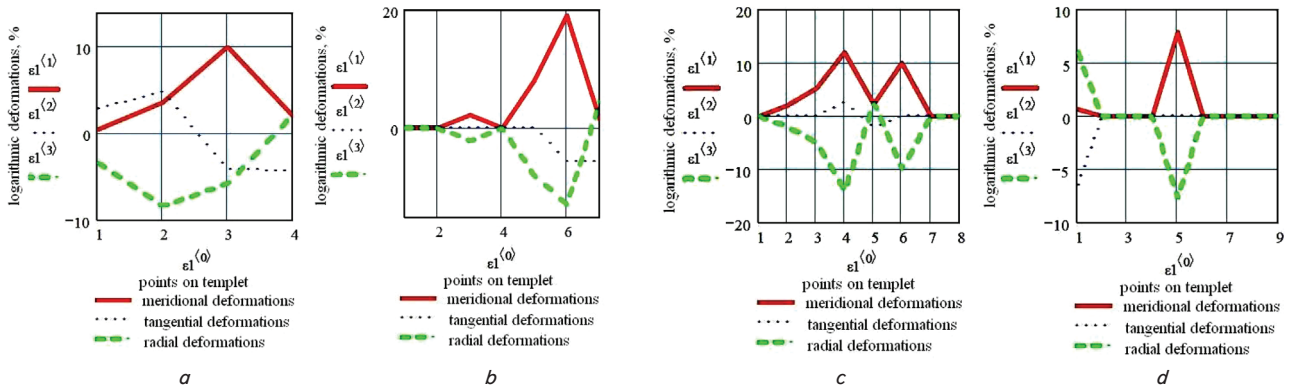


Fig. 10. Standard graphs of distribution of integral logarithmic deformations (meridional, tangential, radial) in the transitions of radial rotary profiling of the wheel rim DW14Lx38: a – 1<sup>st</sup> transition – DW14Lx38; b – 2<sup>nd</sup> transition – DW14Lx38; c – 3<sup>rd</sup> transition – DW14Lx38; d – 4<sup>th</sup> transition – DW14Lx38

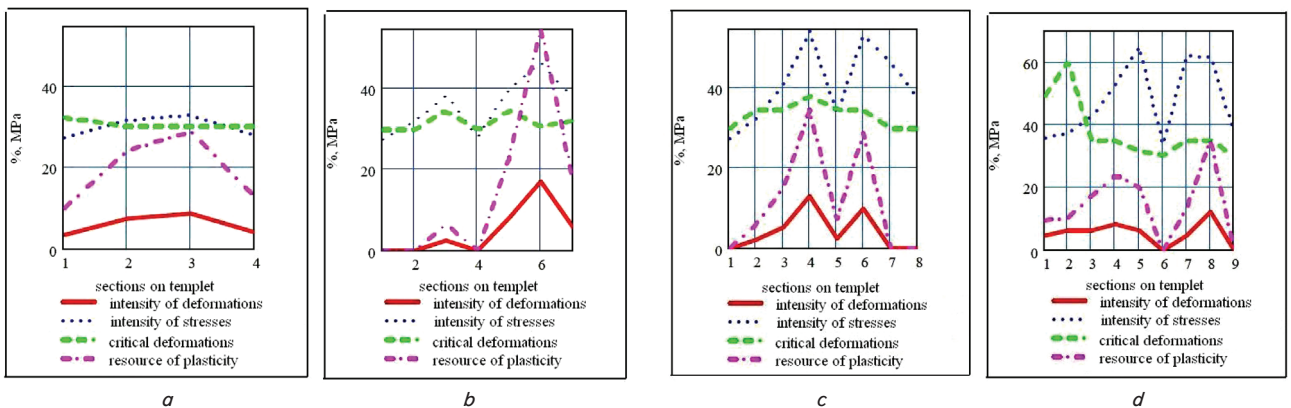


Fig. 11. Standard graphs of distribution of intensities of deformations and stresses, critical deformations and resource of plasticity in the transitions of radial rotary profiling of the wheel rim DW14Lx38: a – 1 transition – DW14Lx38; b – 2 transition – DW14Lx38; c – 3 transition – DW14Lx38; d – 4 transition – DW14Lx38



The second transition of radial-rotary profiling leads to further deformation of each section of the profile. The places of couplings of central stream with its walls are exposed to the largest tensile deformations in the meridional and compressions in the radial directions (point 4, Fig. 9, *a-c*). This is connected to the molding of the section of the workpiece, which, in the previous transition, obtained strengthening and has lower plastic characteristics for both schemes of profiling.

Thus, the intensity of deformations in section 4 of the central stream (Fig. 9, *a-c*) in the end of the first transition of profiling amounted to (4.1 %), (3.9 %) and (4.2 %) for W8x16, 4.5Ex16, 5.5Fx20, respectively, the intensity of stresses – 310MPa, 306MPa и 315MPa, the use of resource of plasticity – (5 %), (5.7 %) and (6.1 %). Further formation of central stream leads to the critical use of the resource of plasticity for this section. This is expressed by excessive thinning of metal in the zones of radius transitions of the central stream to the walls, which sometimes exceed 20 % of its initial thickness. This thickness of metal is not acceptable from the positions of the uniform strength of the rim while operating. In the end of the second transition of profiling the use of the resource of plasticity for the wheel rim W8x16 – (27 %), for 4.5Ex16 – (34.7 %), for 5.5Fx20 – (30.3 %) (point 4 of the templet, Fig. 9, *a-c*). Taking into account the deformations, which this section obtained in the first operation, the total use of the resource of plasticity amounted to: W8x16 – (32 %), 4.5Ex16 – (40.4 %), 5.5Fx20 – (36.4 %).

The repeated deformation of these zones in the third transition of profiling can lead not only to the increased thinning, but also to destruction of the semifinished product.

In the third transition of radial rotary profiling, the remolding of the radius couplings of profile is achieved, from a larger radius to the smaller that correspond to the drawing of the finished product, and the final formation of lateral flanges occurs. The measurement of deformations near the ends of the semifinished product in the third transition revealed that these zones (point 1, Fig. 9, *a-c*) are exposed to the stretching meridional and compressive tangential deformations. This leads to the thickening of metal in the zone of ends of the flanges, in comparison with the previous transitions. The total radial deformation after three transitions of profiling for the wheel rim W8x16 reached:  $(-4.6 - 6.4 + 7 = -4 \%)$ ; for the rim 4.5Ex16:  $(-4.3 - 6.3 + 7 = -3.6 \%)$ ; for the rim 5.5Fx20:  $(-4.0 - 5.6 + 7.5 = -2.1 \%)$ . For example, if the initial thickness of metal of the workpiece in the zone of the end of the lateral flange of the wheel rim 4.5Ex16 was within the limits of 3.5 mm, then its decrease was equal to 0.126 mm. Final thickness after deformation in this zone will reach  $\approx 3.4$  mm, which indicates sufficient hardness of the lateral flange.

Section 3 (Fig. 9, *a-c*) of the coupling of the wall of board flange with the landing shelf in the final stage of profiling is reformed to the coupling with a smaller bending radius in comparison with the previous transition (for the rims 4.5Ex16 and 5.5Fx20). In this zone the stretching meridional and radial deformations occur, tangential are equal to zero, and in some cases, if the coupling is formed in the previous transition, then all three deformations are absent (for the wheel rim W8x16). In any case, this section is exposed to the largest alternating strains in the first and second operation, when the landing shelves are formed. The total radial deformation of this zone: for W8x16 (point 1 (the first transition), point 2 (the second transition), point 3 (the third transition) on templets, Fig. 9, *a*):  $(-4.6 - 8.3 - 0 = -12.9 \%)$ ;

4.5Ex16 (point 3 (the first transition), point 2 (the second transition) and point 3 (the third transition) on templets, Fig. 9, *b*):  $(-9 - 7.5 - 9.8 = -26.3 \%)$ ; 5.5Fx20 (point 3 (the first transition), point 2 (the second transition) and point 3 (the third transition) on templets, Fig. 9, *c*):  $(-8.5 - 7.7 - 9.8 = -26 \%)$ .

The zone of coupling of the landing shelf with the wall of the central stream (points 2, 3, 4 for W8x16 and points 3, 4 for 4.5Ex16 and 5.5Fx20, Fig. 9, *a-c*) is exposed to compression strain in the radial direction in all three transitions for the wheel rim W8x16 and two transitions for the rims 4.5Ex16 and 5.5Fx20. The total radial deformation for W8x16:  $-6.8 - 13 - 1.9 = -21.7 \%$ ; for 4.5Ex16:  $-15 - 1.9 = -16.9 \%$ ; for 5.5Fx20:  $-13 - 1.9 = -14.9 \%$ .

Final profiling of the zone of stream and its couplings with the walls is completed in the third transition of profiling (points 2, 4, 5 – W8x16; points 4, 5 – 4.5Ex16, 5.5Fx20, Fig. 9, *a-c*). The radial deformations are equal to: W8x16:  $-10 - 15 - 2.1 = -27.1 \%$ ; 4.5Ex16:  $-17 - 2.1 = -19.1 \%$ ; 5.5Fx20:  $-15 - 2.7 = -17.7 \%$ . The intensities of stresses for the section of coupling of the wall and the central stream: W8x16 – 471 MPa; 4.5Ex16 – 497 MPa; 5.5Fx20 – 479 MPa.

Generalizing the results of the studies on the stress-strained state when profiling of the narrow-profile rims of wheels, it is possible to draw a conclusion that the largest deformations act on the places of radius couplings of the profile, deformations increase from one transition to the next and their total magnitude can exceed the permitted by 20 % from the initial thickness of the workpiece. Both schemes of the radial rotary profiling: 1 – formation of the central stream and 2 – formation of the shelves are equivalent, although the obtained results testify to the preferability of the second scheme over the first. This coincides with the results of theoretical studies regarding the stresses that act in the process of deformation of the cowling in the transitions where the couplings of the wall and the central stream are exposed to the largest stretching deformations [15, 16].

It was assumed previously [5] that with the formation of wide stream in the first operation (the second scheme), thinning in the couplings of profile will be less than when profiling the narrow stream (the first scheme). However, based on the conducted research, the connection was not established between the width of the stream and the degree of thinning in the places of radius couplings of the profile for the narrow-profile rims of wheels.

When profiling the wide-profile rims of the wheels of standard sizes DW14Lx38 and DW20Ax26, the similar pattern is observed of the distribution of integral logarithmic deformations, stresses, as well as their intensities.

In the first transition, the largest logarithmic compression radial deformation acts on the zone of point 2 for DW14Lx38:  $(-8.4 \%)$  and the zone of point 3 for DW20Ax26:  $(-7.6 \%)$  (Fig. 9, *d, e*). These are the places of couplings of bastings of board flanges with the walls of the stream and the walls with the central stream, respectively. The resource of plasticity for these zones is 12.1 % and 17.3 %. Although the radial deformation for the zone of the point 3 DW20Ax26 is less [3], but in this case, the resource of plasticity proves to be larger because of the action of large plastic deformations in other directions. Hence, it follows that in order to decrease thinning of metal in the radius couplings, it is necessary to seek the heteronymic scheme of the strained state in the meridional and tangential directions.

The second transition of the radial rotary profiling of the wheel rim DW14Lx38 is intended for formation of zone of the central stream, wheel rim DW20Ax26 – formation of zones of the board flanges. The radial logarithmic deformation (the largest in absolute magnitude) affects zones of radius couplings from the wall of the central stream to the stream:  $\varepsilon_r = -13\%$  for DW14Lx38;  $\varepsilon_r = -16\%$  for DW20Ax26. Judging by the given results, the molding of the central stream appears more preferable before the molding of the board flanges.

In the third operation, the lateral flanges for the rim DW14Lx38 are formed, as well as the central stream for DW20Ax26. The largest radial deformations in this transition of profiling are obtained by (Fig. 9, *d, e*): zone 4 of the rim DW14Lx38: ( $-14\%$ ); zones 4, 7, 13 for the rim DW20Ax26: ( $-14\%$ ), ( $-15\%$ ), ( $-14\%$ ). The total radial deformation will be equal to (Fig. 9, *d, e*): for zone 4 of the rim DW14Lx38 (with point 3 of the previous transition): ( $-2.2 - 14 = -16.2\%$ ); for the rim DW20Ax26, point 1: ( $-3.5 - 6.9 = -10.4\%$ ); point 3: ( $-7.2 - 14 - 5.4 = -26.6\%$ ); point 4: ( $-7.6 - 16 + 0 = -23.6\%$ ). When forming the central stream of the rim DW14Lx38 in the second transition (points 6, 7, Fig. 9, *e*), the radial deformations are equal to ( $-8\%$ ) and ( $-13\%$ ), respectively, for the rim DW20Ax26 in the third transition (points 6, 7, Fig. 9, *d*): ( $-11\%$ ) and ( $-15\%$ ).

As can be seen from the given results, during profiling of the central stream, radial deformations prove to be larger for DW20Ax26 as this is connected with the simultaneous deformation of zones of the lateral flanges and the central stream. This leads to an increase in tensile meridional stresses and their localization in the places of radius couplings of the profile, although during profiling of the central stream of the rim DW14Lx38, the deformation affects the sections of the landing shelves. Obviously, tensile meridional stresses, acting in the critical section, have larger magnitude for the rim DW20Ax26 in connection with the larger ration of width of the profile to the diameter, other conditions being equal. The total radial deformation for zone of the central stream amounted to: for DW14Lx38, the coupling of the landing shelf with the wall of the central stream: ( $-8-10-4.6 = -22.6\%$ ); walls with the stream: ( $-13+0-12 = -25\%$ ); for DW20Ax26, the coupling of the landing shelf with the stream: ( $-11-7.9 = -18.9\%$ ); the coupling of walls with the central stream: ( $-15-8.9 = -23.9\%$ ).

The conducted studies and comparison of the results indicates that the application of scheme of profiling the landing shelves, and then zone of the central stream, is more preferable for the wide-profile wheels by the criterion of permissible thinning.

During the radial rotary profiling of the rims of wheels with  $15^\circ$  shelves, we receive similar results on thinning of metal in the places of radius couplings. The largest radial compression strains are observed at the end of the work-piece ( $-9.7\%$ ) and in transition of the landing shelf to the walls of the central stream ( $-9\%$ ).

In the second transition of profiling:

- zone of the end ( $-6.6\%$ );
- coupling of shelves with walls ( $-6\%$ );
- coupling of wall with central stream ( $-9\%$ ).

In the third operation:

- zone of the end ( $+6.0\%$ ); section of coupling shelf to wall  $0\%$ ;
  - zone of radius of bending of the central stream ( $-7.8\%$ ).
- Total radial deformations in all transitions (Fig. 9, *f*):
- zone 1 – ( $-9.7-6.6+6 = -10.3\%$ );

- zone 2 – ( $-9-6+0 = -15\%$ );
- zone 3 – ( $-5,6-9-7.8 = -22.4\%$ ).

The largest radial compression strain is obtained by the section of coupling of the central stream with its wall ( $-22.4\%$ ), while the zone of coupling shelves with the walls ( $-15\%$ ).

If we compare thinning in the similar zones of the profiles of other standard sizes (W8x16 ( $-20.8\%$ ); 4.5Ex16 ( $-17\%$ ); 5.5Fx20 ( $-15\%$ )), then it is possible to draw a conclusion that manufacturing this section of the profile is more expedient to conduct in two transitions, moreover, the largest deformation is to be accomplished in the first transition.

It also follows from the conducted studies that the radial logarithmic compression strain must be average while the meridional and tangential – extreme, and, in order not to observe thinning of metal in dangerous places of the profile, it is necessary that the compressive extreme deformations are the largest by the module. This is possible to achieve during profiling of the central stream in the first transition to the entire designed depth but with the increased radii of bending of the conjugated sections. It is also desirable, if technological process allows it, to perform the shape changing of each design section of the profile separately, which will make it possible to conduct the process of deformation under more favorable conditions, gradually drawing the outlying sections into the deformation area, thus decreasing dangerous stretching meridional deformations.

---

## 7. Conclusions

---

1. The largest logarithmic radial compression strains act on the zones of bending radii from the shelves of the central stream to the central stream both for the narrow-and wide-profile standard sizes of the rims of wheels. The obtained data partially agree with the articles [15, 16] on the examined question. All sections of the rim undergo, in each transition, increasing logarithmic deformations. Generalized results show that the deformations in radius transitions of the final profile are distributed unevenly. In the place of transition from the board to the landing shelf, maximal thinning reaches  $19...21\%$ , elongation  $1...2\%$ , deformation by width  $18...19\%$ . In the zone of transition from the landing shelf to the wall of the central stream, maximal thinning amounts to  $14...15\%$ , elongation  $0\%$ , deformation by width  $15...16\%$ . In radius transitions of the central stream, maximal thinning reaches  $25...29\%$ , elongation  $4\%$ , deformation by width  $29...34\%$ . The maximal intensities of deformations and stresses in the last operation are  $28...37\%$  and  $390-510$  MPa and occur in radius transition of the central stream. The use of resource of plasticity for these zones –  $30...45\%$ .

2. The largest logarithmic deformations are received by the zones of couplings of landing shelves with the walls of the central stream and the walls of the central stream with the central stream for all standard sizes of the rims of wheels. For the rims of wheels W8x16 and DW14Lx38, the second transition of profiling introduces essential effect on the total deformation of these zones: ( $-13\%$ ) and ( $-10\%$ ) for the coupling of the shelf with the walls of the central stream, respectively. For the section of coupling of the walls with the central stream: ( $-15\%$ ) and ( $-13\%$ ). The rims of standard sizes 4.5Ex16, 5.5Fx20 and DW20Ax26 receive the largest deformations of these sections in the first transition of



profiling: (–15 %), (–13 %) and (–11 %) for the connection of the shelf and the wall of the central stream, respectively. For the section of coupling of the wall with the central stream: (–17 %), (–15 %) and (–15 %). The given results testify to different effect of the schemes of profiling on the strain distribution in the transitions.

3. No essential difference between the two schemes of profiling the rims of wheels was revealed:

1 – molding of bastings of the board flanges with the consequent profiling of the central stream;

2 – molding of the central stream with the subsequent molding of the board flanges.

For the narrow-profile rims of wheels, the second scheme is more preferable, for the wide-profile – the first (the best scheme was selected as the one, in which the lowest radial compression strains in the critical cross sections of the profile were observed).

4. The reason for uneven strain distribution along the width of the profile is the drawbacks in the existing schemes of profiling.

For improving technological process of radial rotary profiling for manufacturing the rims of wheels with the lowest metal content, it is necessary, for each standard size of the rim to be considered individually, taking into account the geometry of the workpiece, design dimensions of finished product, the type of steel. For decreasing the magnitude of radial compression deformations, which lead to the thinning of the profile, it is necessary to exclude a possibility of repeated profiling by the same radii (working principle «radius to radius»). Reduction on the rim width should also be redistributed, thus ensuring a gradual shift of angular radius zones from the center to the periphery, to align deformations in the transitions and to provide additional force action on the area of plastic deformation.

## References

1. Wang, X. Effect of forming parameters on sheet metal stability during a rotary forming process for rim thickening [Text] / X. Wang, L. Li, L. Deng, J. Jin, Y. Hu // *Journal of Materials Processing Technology*. – 2015. – Vol. 223. – P. 262–273. doi: 10.1016/j.jmatprotec.2015.04.009
2. Jin, J. A sheet blank rotary forging process for disk-like parts with thickened rims [Text] / J. Jin, X. Wang, L. Li // *Journal of Mechanical Science and Technology*. – 2016. – Vol. 30, Issue 6. – P. 2723–2729. doi: 10.1007/s12206-016-0534-6
3. Bi, D. S. Numerical Simulation on spinning forming process of automotive wheel rim [Text] / D. S. Bi, G. Yang, L. Chu, J. Zhang, Z. H. Wang // *Materials Science Forum*. – 2012. – Vol. 704–705. – P. 1458–1464. doi: 10.4028/www.scientific.net/msf.704-705.1458
4. Dragobekij, V. Uchet vlijaniya izmeneniya tolshhiny listovoj zagotovki v processe deformirovaniya [Text] / V. Dragobekij, A. Zjukov, A. Konovalenko // *Visnik Kremenuch'kogo derzhavnogo politehničnogo universitetu: Naukovi praci KDPU*. – 2005. – Vol. 2. – P. 61–62.
5. Potekushin, N. Jeksperimental'noe issledovanie processa formoobrazovaniya profilirovannyh obod'ev [Text] / N. Potekushin // *Avtomobil'naja promyshlennost'*. – 1977. – Vol. 1. – P. 33–36.
6. Currie, A. Finite Element Analysis of an Automotive Wheel [Text] / A. Currie // *A Case Study, National Conference Publication*, 2000. – P. 16–20.
7. Conceicao Antonio, C. A. Optimal design of beam reinforced composite structures under elasto-plastic loading conditions [Text] / C. A. Conceicao Antonio, J. Trigo Barbosa, L. Simas Dinis // *Structural and Multidisciplinary Optimization*. – 2000. – Vol. 19. – P. 50–63. doi: 10.1007/s001580050085
8. Ray, G. S. Profile optimisation of variable thickness rotating discs [Text] / G. S. Ray, B. K. Sinha // *Computers & Structures*. – 1992. – Vol. 42, Issue 5. – P. 809–813. doi: 10.1016/0045-7949(92)90191-2
9. Mori, K. Simulation of three dimensional rolling by the rigid-plastic finite element method [Text] / K. Mori, K. Osakada // *Numerical methods in industrial forming processes: proc. International Conf.*, 1982. – P. 747–756.
10. Kasatkin, B. Jeksperimental'nye metody issledovaniya deformatsij i naprjazhenij [Text] / B. Kasatkin, A. Kudrin, L. Lobanov. – Kyiv: Naukova dumka, 1981. – 583 p.
11. Ogorodnikov, V. A. Vybór kriteriev deformiruемости pri ocenke ispol'zovannogo resursa plastichnosti v processah obrabotki metallov davleniem [Text] / V. A. Ogorodnikov, A. V. Grushko, A. V. Gucaljuk // *Visnik NTU «HPI»*. – 2014. – Vol. 43. – P. 127–136.
12. Romanovskij, V. Spravočnik po holodnoj shtampovke [Text] / V. Romanovskij. – Leningrad: Mashinostroenie. Leningrad: otd-nie, 1979. – 520 p.
13. Tret'jakov, A. Mehanicheskie svojstva stalej i splavov pri obrabotke davleniem [Text] / A. Tret'jakov, V. Zjuzin. – Moscow: Metallurgija, 1973. – 224 p.
14. Glushhenkov, V. Uprochnenie metallov v obrabotke metallov davleniem [Text] / V. Glushhenkov. – Samara: SGAU, 2010. – 33 p.
15. Puzyr, R. Distribution analysis of stresses across the stretching edge of die body and bending radius of deforming roll during profiling and drawing of cylindrical workpiece [Text] / R. Puzyr, D. Savelov, R. Argat, A. Chernish // *Metallurgical and Mining Industry*. – 2015. – Vol. 1. – P. 27–32.
16. Puzyr, R. Raschet komponent tenzora naprjazhenij na radiuse zakruglenija profilirujushhego rolka pri izgotovlenii oboda kola [Text] / R. Puzyr // *Obrabotka materialov davleniem*. – 2015. – Vol. 2. – P. 192–195.
17. Savelov, D. Peculiarities of vibrational press dynamics with hard-elastic restraints in the working regime of metal powders molding [Text] / D. Savelov, V. Dragobetsky, R. Puzyr, A. Markevych // *Metallurgical and Mining Industry*. – 2015. – Vol. 2. – P. 67–75.